Enhanced Nonlinear Effects in Metamaterials and Plasmonics

Christos Argyropoulos, Pai-Yen Chen, and Andrea Alù

Department of Electrical and Computer Engineering, The University of Texas at Austin
1 University Station C0803, Austin, TX 78712, USA
*corresponding author: alu@mail.utexas.edu

Abstract

In this paper we provide an overview of the anomalous and enhanced nonlinear effects available when optical nonlinear materials are combined inside plasmonic waveguide structures. Broad, bistable and all-optical switching responses are exhibited at the cut-off frequency of these plasmonic waveguides, characterized by reduced Q-factor resonances and extended enhancement volumes. These phenomena are due to the large field enhancement obtained inside specific plasmonic gratings, which ensures a significant boosting of the nonlinear operation. Several exciting applications are proposed, which may potentially lead to new optical components and add to the optical nanocircuit paradigm.

1. Introduction

The research fields of plasmonics and metamaterials have led to a series of exciting applications in optics, such as subwavelength imaging [1], the cloak of invisibility [2], [3] and ε -near-zero (ENZ) materials [4], [5]. The linear operation of these devices has been widely studied during the last years and successfully implemented experimentally [6]-[11]. Novel directions to optical metamaterial research are offered by the inclusion of gain [12] and nonlinear materials [13]-[14] into the picture.

In this work, we mainly focus on an overview of the wave interaction of third-order Kerr nonlinear $\chi^{(3)}$ materials loaded in plasmonic metamaterial waveguides. Dielectric Kerr materials generally exhibit weak nonlinearities at optical frequencies, with maximum values in the order of $10^{-20} m^2 / V^2$ [15]. In the past, several research studies have focused on enhancing these weak third-order nonlinear effects based on plasmonic structures. For instance, Kerr nonlinear materials may be loaded at the gap of plasmonic nanoantennas to achieve stronger nonlinear effects, such as optical bistability and efficient all-optical switching [16]-[17]. The strong resonant fields confined at the nanoantenna's gap are the main reason of the boosted nonlinear performance. Nevertheless, these effects are based on narrowband resonant operation characterized by high Qfactors. Even more importantly, the strongly enhanced fields are confined to an extremely small volume at the gap of the nanoantenna, a fact that limits the actual size of the effectively enhanced Kerr material, limiting the overall nonlinear performance.

Alternative approaches to increase third-order nonlinear effects have been based on plasmonic gratings [18]-[19] and exotic metamaterial structures [20]. Again, all these works suffer from narrowband operation (high Q-factor resonances) and limited volumes. In particular, the authors in [18] have proposed to use the extraordinary optical transmission (EOT) concept [21] to achieve broad optical bistability. EOT is based on Fabry-Perot (FP) constructive wave interference, leading to a well-known standing wave distribution in the slits. All these resonant phenomena base the nonlinearity enhancement on field localization and, as in Purcell effect, support high Q-factors, small volumes and narrow bandwidths to achieve stronger nonlinearity enhancement.

Here, we propose a different way to achieve strong optical nonlinearities, combining lower Q-factors and a larger available volume over which the nonlinear effect may be increased. An ideal field configuration to efficiently boost optical nonlinear effects would require strong, highly confined, homogeneous electric fields with uniform phase over a large volume. All of these properties surprisingly exist in certain ENZ metamaterial structures. The quasistatic field distribution inside an ENZ channel can provide highly enhanced homogeneous fields combined with constant phase distribution [4]-[5]. Moreover, these effects can be realized for elongated, theoretically infinite, channels, whose shape may be bent in arbitrary ways. Phase matching is also achieved at the ENZ operation, a critical advantage towards boosted nonlinearities, especially when exciting electrically large nonlinear samples.

In this paper, we review and present numerical results on the scattering and bistable properties of a threedimensional (3D) array of plasmonic ENZ channels standing in free-space, a geometry firstly presented in [22]. Inside these plasmonic waveguides, ENZ and FP tunneling can be obtained in distinct frequency regimes, allowing an easy comparison between the two methods to enhance the nonlinear response of Kerr materials. The ENZ resonance is realized at the cut-off frequency of the slits, as it will be discussed in the following, a function of the transverse dimension of the slits, i.e., their width. On the contrary, the FP resonances arise at higher frequencies, when the longitudinal dimension of the slits, i.e., their length, is proportional to half of the guided wavelength in the slit. Note that the proposed structure is different from the one proposed in [18], where only FP resonances are supported, since the slits were 2-D, without cut-off. We introduce Kerr nonlinear materials inside the plasmonic channels and we verify that at the ENZ frequency regime stronger bistable effects are obtained compared to FP tunneling [22]. More importantly, we explicitly demonstrate that broad bistability and strong all-optical switching can be obtained at the ENZ operation, which is characterized by reduced Q-factor resonances, different to other available techniques for plasmonic enhanced optical nonlinearities [17]-[20]. Finally, the effective permittivity at the cut-off frequency of the array of plasmonic waveguides is also derived. We demonstrate that the proposed plasmonic grating constitutes an artificial nonlinear metamaterial with ENZ linear properties and drastically enhanced nonlinear properties. This unconventional response opens the possibility to modulate from low-positive to low-negative values the effective permittivity, as a function of the applied intensity and of the type of loaded third-order nonlinear material. We envision novel optical nonlinear devices inspired by the proposed structure, such as self-tunable slow-light devices, low-intensity optical memories, switches and tunable sensors.

2. Theoretical analysis of the problem

The geometry of the plasmonic geometry under study is depicted in Fig. 1. Narrow rectangular apertures loaded with third-order $\chi^{(3)}$ Kerr nonlinear optical materials are carved in a thick silver (Ag) screen. The design parameters are chosen to be: height t=40nm, width w=200nm, length l=500nm and periods a=b=400nm. These dimensions are selected in order to obtain the ENZ frequency close to first and second FP resonances, in order to be able to clearly compare their performance, as it will be shown later in the paper. Note that the height of the channels is chosen much smaller than their width t=w and the periods are selected a,b? t with the aim to achieve stronger field confinement at the ENZ operation [5].

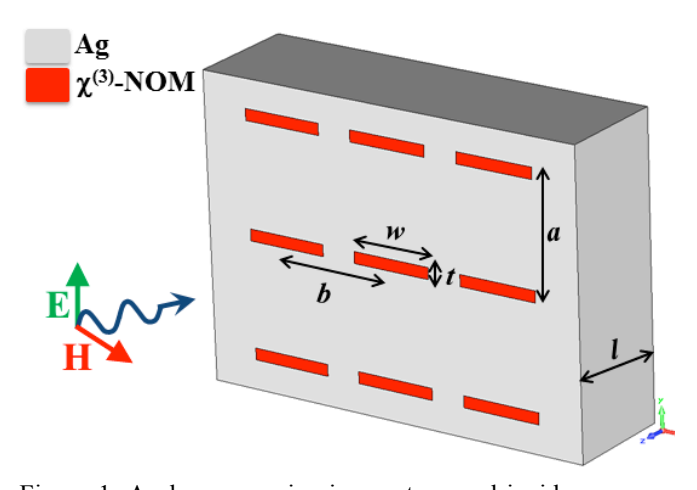


Figure 1: A plane wave impinges at normal incidence on a nonlinear ENZ metamaterial slab. Narrow rectangular apertures loaded with third-order Kerr nonlinear optical materials (red) are carved in an elongated silver screen (light grey).

The slab is composed of Ag and has a relative permittivity which follows the Drude dispersion model at optical frequencies $\varepsilon_{Ag} = \varepsilon_{\infty} - f_p^2 / \left[f \left(f + i \gamma \right) \right]$, $f_p = 2175\,\mathrm{THz},\ \gamma = 4.35\,\mathrm{THz},\ \varepsilon_{\infty} = 5\,$ [23]. The apertures are loaded with Kerr nonlinear material with a relative permittivity $\varepsilon_{ch} = \varepsilon_L + \chi^{(3)} \left| E_{ch} \right|^2$. The linear permittivity is chosen $\varepsilon_L = 2.2$ and the nonlinear susceptibility $\chi^{(3)} = 4.4 \times 10^{-20} \, m^2 / V^2$. These are typical values for nonlinear optical materials [15]. Finally, the magnitude of the localized electric field inside the elongated channels is depicted as $\left| E_{ch} \right|$.

The dominant transmitted mode in this type of rectangular plasmonic waveguides is quasi-TE₁₀. It 'feels' an effective near-zero permittivity when we operate at the cut-off frequency of the plasmonic channels. In our previous works [5],[22], we derived a rigorous homogenization model to describe the effective permittivity of the nonlinear structure shown in Fig. 1. The effective permittivity is given by the formula

$$\varepsilon_{eff} = \frac{\beta_{pp}^2}{k_0^2} - \frac{\pi^2 \varepsilon_{ch}}{\left(\beta_{pp} w + 2\sqrt{\varepsilon_{ch}} / \sqrt{\text{Re}\left[-\varepsilon_{Ag}\right]}\right)^2},$$
 (1)

where β_{pp} is the guided wavenumber in the associated parallel-plate plasmonic waveguide with the same height t as the apertures, but infinite width [24]. Equation (1) is also dependent to the permittivity of the material loaded inside the slits ε_{ch} , the silver's permittivity ε_{Ag} and the width w of the plasmonic waveguides. In the limit $\varepsilon_{Ag} \rightarrow -\infty$ (Ag substituted by a perfect conductor) and $\beta_{pp} = k_0 \sqrt{\varepsilon_{ch}}$, Eq. (1) takes the simple form

$$\varepsilon_{\text{eff}} = \varepsilon_{ch} - \left(\frac{\pi}{k_0 w}\right)^2 \tag{2}$$

and the classic cut-off condition $w = \pi/(k_0 \sqrt{\varepsilon_{ch}})$ is obtained to achieve zero effective permittivity $\varepsilon_{eff} = 0$. The nonlinear Kerr permittivity may be substituted in the channel permittivity in Eq. (2) and an elegant and compact formula may be derived for the effective permittivity of the slab:

$$\varepsilon_{\text{eff}} = \varepsilon_L - \frac{\pi^2}{k_0^2 w^2} + \chi^{(3)} \left| E_{ch} \right|^2. \tag{3}$$

At the quasi-static ENZ operation, the enhanced electric field inside the slits can be directly evaluated using power conservation at the discontinuities in the E and H planes of the grating [22]. It varies only with the geometric parameters of the plasmonic channels and the incident electric field, providing the following result:

$$E_{ch} = \frac{(ba)}{(tw)} E_{in}. \tag{4}$$

Hence, Eq. (4) may be substituted in Eq. (3) to obtain the general formula for the effective permittivity of the nonlinear metamaterial slab shown in Fig. 1 as a function of the structure's geometry, nonlinear material parameters and input intensity:

$$\varepsilon_{eff} = \varepsilon_L - \frac{\pi^2}{k_0^2 w^2} + \frac{b^2 a^2}{w^2 t^2} \chi^{(3)} |E_{in}|^2.$$
 (5)

Equation (5) explicitly describes the effective permittivity of the nonlinear metamaterial of Fig. 1 at its ENZ operation. The proposed nonlinear structure has very interesting properties: first, it can realize an enhanced effective nonlinear susceptibility, which varies only with the geometrical parameters of the structure and it is equal to

$$\chi_{eff}^{(3)} = \left(\frac{ba}{wt}\right)^2 \chi^{(3)}.$$
 (6)

As a result, the effective nonlinearity in the current geometry at the ENZ resonance is strongly enhanced: $\chi_{eff}^{(3)} = 400 \chi^{(3)}$. Furthermore, at the cut-off frequency (ENZ operation) $\varepsilon_L = \pi^2/(k_0 w)^2$. The corresponding effective permittivity varies only with its nonlinear part in Eq. (5), and it is given by the simple formula:

$$\varepsilon_{\text{eff}} = \frac{b^2 a^2}{w^2 t^2} \chi^{(3)} |E_{in}|^2.$$
 (7)

Equation (7) clearly shows that the proposed metamaterial design can inherently modulate its effective permittivity by simply changing the nonlinear susceptibility of the material or the structure's geometry. It can lead to positive or negative values of effective permittivity, when focusing nonlinearities $\chi^{(3)} > 0$ or defocusing nonlinearities $\chi^{(3)} < 0$ are considered, respectively.

The aforementioned concept is graphically depicted in Fig. 2(a). It is obvious that the effective permittivity can take positive/negative values with a maximum/minimum value of ± 0.4 when focusing/defocusing nonlinearities are loaded inside the slits of the metasurface. In a similar way, the effective permittivity versus the input optical intensity is plotted in Fig. 2(b). Now, a linear curve is obtained due to the relationship: $I_{in} = \left|E_{in}\right|^2/2\eta_0$, where η_0 ; 377 Ω is the free-space impedance. The proposed artificial nonlinear metamaterial can have plenty of interesting applications for metamaterials, such as novel slow-wave devices, modulators and nonlinear cloaking coatings [25].

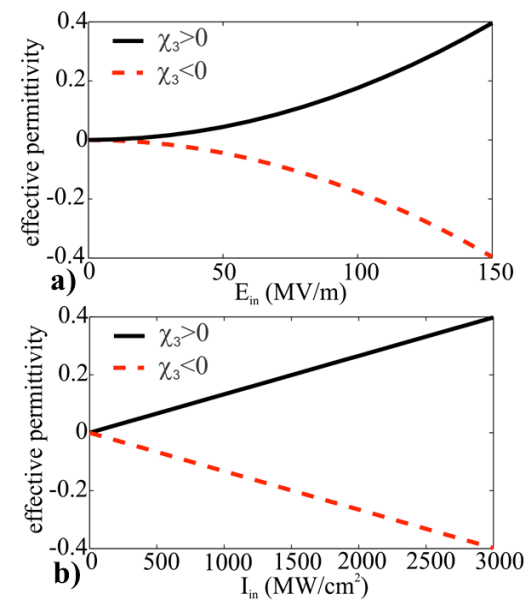


Figure 2: The effective permittivity of an artificial nonlinear ENZ metamaterial as in Fig. 1, as a function of: (a) the input electric field and (b) the input optical intensity. Positive values of effective permittivity are obtained for focusing nonlinearities $\chi^{(3)} > 0$ (black solid lines) and negative values for defocusing nonlinearities $\chi^{(3)} < 0$ (red dashed lines) for both figures.

3. Linear and nonlinear operation

First, we study the linear operation, when linear dielectrics are loaded inside the slits of Fig. 1 or moderate intensities are considered. The material loaded in the channels has $\chi^{(3)} = 0 \rightarrow \varepsilon_{ch} = \varepsilon_L = 2.2$. permittivity transmission coefficient of the proposed structure is computed with rigorous full-wave simulations based on finite-integration technique and employing commercially available software [26]. The transmission coefficient of the structure as a function of frequency is plotted in Fig. 3. The first transmission peak is found around $f_{ENZ} = 295 THz$ and it corresponds to the cut-off frequency of the plasmonic rectangular waveguide. This peak is independent of the channel's length and it has a moderate Q-factor $Q_{\text{\tiny ENZ}}$; 48. Two distinct resonances follow the ENZ operation, which correspond to the first and second FP frequency regimes. They are found at approximately $f_{FP1} = 322 \, THz$ and $f_{FP2} = 384THz$ for the current geometry. These resonances depend highly on the channel's length, and they have similar Q-factors as the ENZ operation. Note that, with further optimization of the current geometry, these resonances may be easily tuned to optical frequencies rather than infrared. Moreover, the Q-factor of the ENZ resonance can become even lower, if we further decrease the channel's length [5].

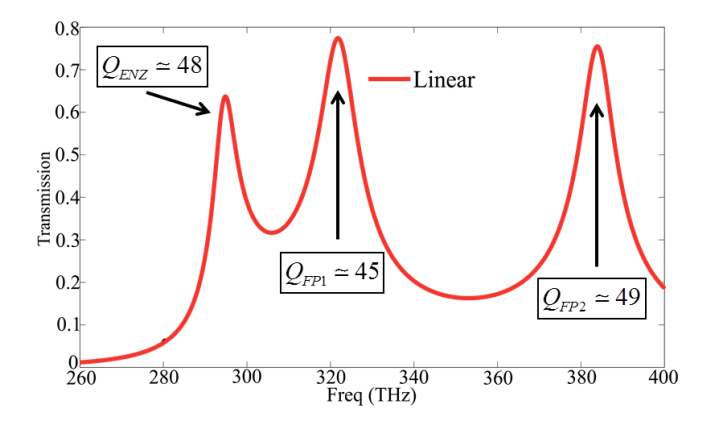


Figure 3: Transmission coefficient versus frequency for linear material loaded in the slits shown in Fig. 1. Three distinct resonances (ENZ, FP 1, FP 2) exist with almost similar, relative low, Q-factors.

Next, the 3D electric field distributions are computed and demonstrated in Fig. 4 inside one plasmonic waveguide slit at the ENZ, first FP and second FP resonances. These distributions further help us to achieve a more in-depth physical understanding of each tunneling mechanism. The field distribution in the ENZ case is drastically different compared to the FP resonances. Homogeneous, highly confined and constant phase fields are obtained at the ENZ frequency [Fig. 4(a)], contrary to the standing wave field distributions of the first and second order FP resonances [Figs. 4(b), (c)]. This explains the reason why the transmission at the ENZ is slightly reduced compared to FP resonances (see Fig. 3). The enhanced homogeneous fields will be more dissipated due to the losses in the silver walls of the plasmonic waveguide. In a similar and even stronger way, we expect that the nonlinear effects will be boosted at the ENZ frequency, when the slits will be filled with Kerr nonlinear media, due to the high total field enhancement.

Now, we load Kerr nonlinear materials inside the slits to study the nonlinear response of the geometry of Fig. 1. The nonlinear transmission versus frequency for a moderate input optical intensity of $I_{in} = 3000 \, MW / cm^2$ is depicted in Fig. 5. It is obvious that a broader bistable performance is obtained at the ENZ operation compared to weaker bistable curves at both FP resonances. This is a direct consequence of the enhanced homogeneous total field at the ENZ operation (the comparison was shown in Fig. 4). Moreover, it is very important to stress that the current broad bistable effects obtained at the ENZ frequency can be achieved with moderate input intensities and with reduced Q-factor resonances, computed before in Fig. 3. In other words, we obtain enhanced nonlinearities by extending the effective volume over which fields are amplified, rather than increasing the Q-factor of the system, as common in conventional Purcell effects. This interesting enhanced nonlinear optical effect is demonstrated for this specific example, but it may be tuned to different frequencies and geometries, as a function of the desired application. We speculate that this phenomenon can directly lead to more practical and efficient optical memories and switches, due to the larger hysteresis available at the ENZ frequency.

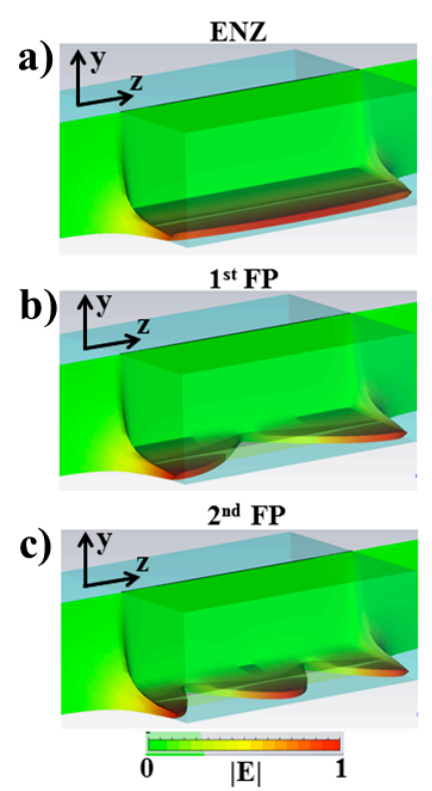


Figure 4: The electric field distributions are computed inside the narrow rectangular apertures at the a) ENZ operation and at the b) 1st FP and c) 2nd FP frequency resonances. Homogeneous and highly confined fields are obtained at the ENZ frequency (a), on the contrary standing wave field patterns are observed at the first (b) and second (c) FP frequencies.

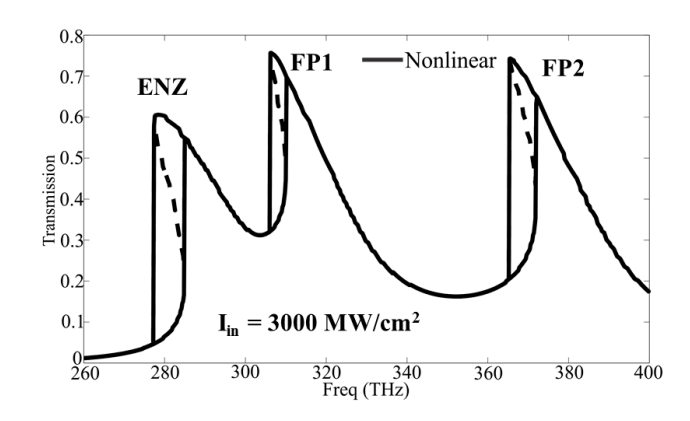


Figure 5: Transmission coefficient versus frequency for the slab nonlinear operation. A strongest hysteresis and bistable response is clearly obtained at the ENZ frequency.

4. Conclusions

In this work, we have demonstrated a robust way to achieve boosted optical nonlinear responses with moderate optical intensities and reduced Q-factor resonances. The design of artificial ENZ metamaterials standing in free-space was proposed and a homogenized formula for its effective permittivity was derived. Interestingly, its performance can be modulated by the type of nonlinear materials introduced inside its apertures. Positive or negative permittivity values can be obtained, with plenty of potential applications in the field of artificially engineered nonlinear metamaterial devices. We believe that the proposed structure can be fabricated within available nanofabrication methods, such as nanoskiving [27]. The peculiar quasi-static properties of effective ENZ media obtained at the metamaterial cut-off were utilized to achieve huge bistable response with a low Q-factor resonance confined in a large spatial extent. Finally, we speculate that in a similar way to nonlinearities, the Purcell factor can be enhanced at the ENZ operation without the usual restrictions of small volumes and high Ofactor resonances [28]. This can have interesting potential applications in future optical nanocircuits and laser designs.

Acknowledgements

This work has been supported by the ONR MURI grant No. N00014-10-1-0942.

References

- [1] J. B. Pendry, "Negative refraction makes a perfect lens," *Phys. Rev. Lett.* 85, 3966, 2000.
- [2] A. Alù, N. Engheta, "Achieving transparency with plasmonic and metamaterial coatings," *Phys. Rev. E* 72, 016623, 2005.
- [3] J. B. Pendry, D. Shurig, D. R. Smith, "Controlling electromagnetic fields," *Science* 312, 1780, 2006.
- [4] M. G. Silveirinha, N. Engheta, "Tunneling of Electromagnetic Energy through Subwavelength Channels and Bends using ε-Near-Zero Materials," *Phys. Rev. Lett* 97, 157403, 2006.
- [5] A. Alù, N. Engheta, "Light squeezing through arbitrarily shaped plasmonic channels and sharp bends," *Phys. Rev. B* 78, 035440, 2008.
- [6] N. Fang, H. Lee, X. Zhang, "Sub-Diffraction-Limited Optical Imaging with a Silver Superlens," *Science* 308, 534, 2005.
- [7] D. Schurig, J. J. Mock, B. J. Justice, S. A. Cummer, J. B. Pendry, A. F. Starr, D. R. Smith, "Metamaterial Electromagnetic Cloak at Microwave Frequencies," *Science* 314, 977, 2006.
- [8] B. Edwards, A. Alù, M. G. Silveirinha, N. Engheta, "Experimental Verification of Plasmonic Cloaking at Microwave Frequencies with Metamaterials," *Phys. Rev. Lett.* 103, 153901, 2009.
- [9] D. Rainwater, A. Kerkhoff, K. Melin, J. C. Soric, G. Moreno, A. Alù, "Experimental Verification of Three-

- Dimensional Plasmonic Cloaking in Free-Space," *New Journ. of Phys.* 14, 013054, 2012.
- [10] B. Edwards, A. Alù, M. E. Young, M. Silveirinha, N. Engheta, "Experimental Verification of Epsilon-Near-Zero Metamaterial Coupling and Energy Squeezing Using a Microwave Waveguide," *Phys. Rev. Lett.* 100, 033903, 2008.
- [11] R. Liu, Q. Cheng, T. Hand, J. J. Mock, T. J. Cui, S. A. Cummer, D. R. Smith, "Experimental Demonstration of Electromagnetic Tunneling Through an Epsilon-Near-Zero Metamaterial at Microwave Frequencies," *Phys. Rev. Lett.* 100, 023903, 2008.
- [12] S. Xiao, V. P. Drachev, A. V. Kildishev, X. Ni, U. K. Chettiar, H.-K. Yuan, V. M. Shalaev, "Loss-free and active optical negative-index metamaterials," *Nature* 466, 735, 2010.
- [13] A. Bouhelier, M. Beversluis, A. Hartschuh, L. Novotny, "Near-Field Second-Harmonic Generation Induced by Local Field Enhancement," *Phys. Rev. Lett.* 90, 013903, 2008
- [14] N. I. Zheludev, "The road ahead for metamaterials," *Science* 328, 582, 2010.
- [15] R. W. Boyd, Nonlinear Optics, Academic, London, 1992.
- [16] V. P. Drachev, A. K. Buin, H. Nakotte, V. M. Shalaev, "Size dependent χ^{3} for conduction electrons in Ag nanoparticles," *Nano Lett.* 4, 1535, 2004.
- [17] P. Y. Chen, A., Alù, "Optical nanoantenna arrays loaded with nonlinear materials," *Phys. Rev. B* 82, 235405, 2010.
- [18] J. A. Porto, L. Martín-Moreno, F. J. García-Vidal, "Optical bistability in subwavelength slit apertures containing nonlinear media," *Phys. Rev. B* 70, 081402(R), 2004.
- [19] G. D'Aguanno, D. Ceglia, N. Mattiucci, M. J. Bloemer, "All-optical switching at the Fano resonances in subwavelength gratings with very narrow slits," *Opt. Lett.* 36, 1984, 2011.
- [20] M. Ren, B. Jia, J.-Y. Ou, E. Plum, J. Zhang, K. F. MacDonald, A. E. Nikolaenko, J. Xu, M. Gu, N. I. Zheludev, "Nanostructured Plasmonic Medium for Terahertz Bandwidth All-Optical Switching," Adv. Mater. 23, 5540, 2011.
- [21] F. J. García-Vidal, E. Moreno, J. A. Porto, L. Martín-Moreno, "Transmission of Light through a Single Rectangular Hole," *Phys. Rev. Lett.* 95, 103901, 2005.
- [22] C. Argyropoulos, P.-Y. Chen, G. D'Aguanno, N. Engheta, A. Alù, "Boosting Optical Nonlinearities in ε-Near-Zero Plasmonic Channels," *Phys. Rev. B* 85, 045129, 2012.
- [23] P. B. Johnson, R. W. Christy, "Optical Constants of the Noble Metals," *Phys. Rev. B* 6, 4370, 1972.
- [24] A. Alù, N. Engheta, "Optical nanotransmission lines: synthesis of planar left-handed metamaterials in the

- infrared and visible regimes," J. Opt. Soc. Am. B 23, 571, 2006.
- [25] C. Argyropoulos, P. Y. Chen, F. Monticone, G. D'Aguanno, A. Alù, "Nonlinear Plasmonic Cloaks to Realize Giant All-Optical Scattering Switching," *Phys. Rev. Lett.* 108, 263905, 2012.
- [26] CST Microwave StudioTM 2011, CST of America, Inc.
- [27] Q. Xu, R. M. Rioux, M. D. Dickey, G. M. Whitesides, "Nanoskiving: A New Method To Produce Arrays of Nanostructures," *Acc. Chem. Res.* 41, 1566, 2008.
- [28] E. M. Purcell, "Spontaneous Emission Probabilities at Radio Frequencies," *Phys. Rev.* 69, 681, 1946.